Journal of Magnetics 17(1), 27-32 (2012) http://dx.doi.org/10.4283/JMAG.2012.17.1.027

Parallel Load Techinques Application for Transcranial Magnetic Stimulation

Sun-Seob Choi[1] and Whi-Young Kim[2]*

[1]*Department of Radiology/ Neuro radiology Section, Dong-A University Medical Center, Busan 602-715, Korea*
[2]*Department of Biomedical Engineering, Dong-ju College University, Busan 602-715, Korea*

(Received 5 November 2011, Received in final form 8 December 2011, Accepted 9 December 2011)

Transcranial magnetic stimulation requires an electric field composed of dozens of V/m to achieve stimulation. The stimulation system is composed of a stimulation coil to form the electric field by charging and discharging a capacitor in order to save energy, thus requiring high-pressure kV. In particular, it is charged and discharged in capacitor to discharge through stimulation coil within a short period of time (hundreds of seconds) to generate current of numerous kA. A pulse-type magnetic field is formed, and eddy currents within the human body are triggered to achieve stimulation. Numerous pulse forms must be generated to initiate eddy currents for stimulating nerves. This study achieved high internal pressure, a high number of repetitions, and rapid switching of elements, and it implemented numerous control techniques via introduction of the half-bridge parallel load method. In addition it applied a quick, accurate, high-efficiency charge/discharge method for transcranial magnetic stimulation to substitute an inexpensive, readily available, commercial frequency condenser for a previously used, expensive, high-frequency condenser. Furthermore, the pulse repetition rate was altered to control energy density, and grafts compact, one-chip processor with simulation to stably control circuit motion and conduct research on motion and output characteristics.

Keywords : half bridge converter, charge, microprocessor, AVR, High Speed, AT80S8535

1. Introduction

Transcranial magnetic stimulation is a method of inducing an electric field within the human body via a temporally varying magnetic field. Since the size of the electric field used in stimulation must be dozens of V/m and the switching time of the unsteady magnetic field must be below hundreds of milliseconds, a pulse magnetic field for human applications must consist of numerous tesla [1,2]. Technology previously used for switching strong magnetic fields within a short time period resulted in a magnetic pulse generation frequency for transcranial magnetic stimulation that was less than dozens of Hz. Thus, transcranial magnetic stimulation was commonly used for diagnosing, rather than treating, various disorders of the nervous system [3, 12]. In particular, it is charged and discharged in capacitor to discharge through stimulation coil in a short period of time (within hundreds of seconds) to generate current of numerous kA [4, 5]. Generation must be achieved in various pulse forms to produce eddy currents for stimulating nerves [6-8].

These functionalities require a high capacity power device, high internal pressure, numerous repetitions, a rapidly switching element, and various control techniques. Regular transcranial magnetic stimulation boosts a 60 Hz power sine wave in order to achieve a high voltage charge of electric current in capacitor. Various constraints include turn ratios of the transformer, power loss, size, system complexity, high voltage, and high current control [9, 10]. This study introduced the half bridge parallel load switching technique, which allows controlled charge-discharge of electric current in the capacitor and can be used to achieve free form voltage and current pulses in order to meet repetition, efficiency, size, weight, and power efficiency requirements. In the half-bridge parallel load method, voltage stress exerted by the switch element possesses the equivalent of input voltage, unlike the forward, push pull method that possesses a switch voltage stress that is twice that of the input voltage [3, 11]. Since the switch operation waveform manifests as a half-wave, symmetric shape, this structure can be extensively used in mid-sized, large capacity convertors. In addition, this study investigated the effect of a secondary output of the stimulation coil by

*Corresponding author: Tel: +82-51-200-3449
Fax: +82-51-200-3235, e-mail: ndyag@dongju.ac.kr

adding a reverse direction circuit to the previous method of a single pulse stimulation coil output. Therefore, this stable method achieves high repetitions, high output, and high efficiency.

2. Design

2.1. Parallel Load Method

Fig. 1 presents the main power device of the transcranial magnetic stimulation used in the resonant converter method. Interpretation is achieved in five sections of discontinuous mode ($0 < f < 0.5_{fn}$) and is also effective in Continuous Mode to be organized according to section. Stage 1 ($0 < t \le t_1$) begins when IGBT-1 is turned on, and the L_r current linearly increases to establish the following relational expression.

$$\frac{di_L(t)}{dt} = \frac{Vs}{2L}t_1 = \frac{2L_R I_o}{Vs} \tag{1}$$

Stage 2 ($t_1 < t \le t_2$) begins when current flowing in L_r becomes identical to Io. Since they supply power from input to output, L_r and C_r are resonated to increase C_r voltage. Voltage increase of C_r acts through a reverse bias in D_4 and D_5 to be turned off, and D_3 and D_6 maintain continuity status using the initial conditions of

$$i_L(0) = Io,\ vc,\ (0) = 0$$

$$i_{Ll}(t) = Io + \frac{Vs}{2Zo}\sin\varpi(t - t_1),\ vc_r(t)$$

$$= \frac{Vs}{2}[1 - \cos\varpi(t - t_1)] \tag{2}$$

In Stage 3 ($t_2 < t \le t_3$), $D1$ flows in the resonating current section, and energy of the resonating circuit is regenerated as input.

$$t_3 = t_1 + \frac{2\pi - \sin^{-1}(2I_o Z_o / V_s)}{\omega_n} \tag{3}$$

Stage 4 ($t_3 < t \le t_4$) Cr becomes non-zero voltage in the t4 point through continuous discharge of resonant energy.

$$v_c,(t) = \frac{1}{C_r}\int_{\wp}^{g} -I_0 dt = vc,(t_3) - \frac{I_o(t - t_3)}{C_r} \tag{4}$$

Stage 5 ($t_4 < t \le t_5$) maintains the turn-off status of IGBT-1 and IGBT-2, and Cr maintains non-zero voltage. Thus, output current achieves reflux status through $D_{3\sim6}$. A cycle can be segmented into six sections. Three sections of the half-cycle are opposite in polarity during continuous mode ($0.5_{fn} < fs < fn$ or below-resonant mode) and below-resonant mode. Stage 1 starts at $t = 0$ when IGBT-1 is turned on, and it ends at t_1 that reaches non-zero voltage by being charged by the addition of L_r current and Io due to negative C_r bi-voltage. Stage 2 is the resonant section and possesses positive C_r bi-voltage. Thus, Io

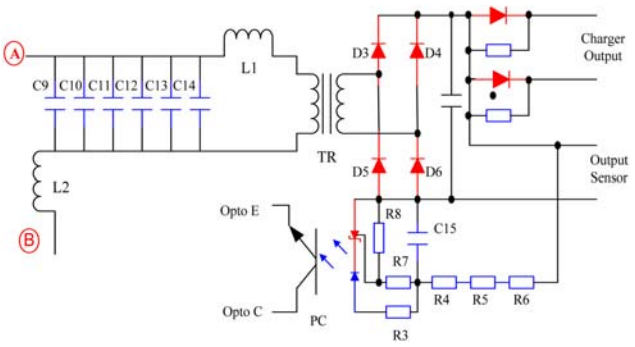

Fig. 2. (Color online) Circuit for monitoring output and the output sensor of the charge-discharge through the capacitor.

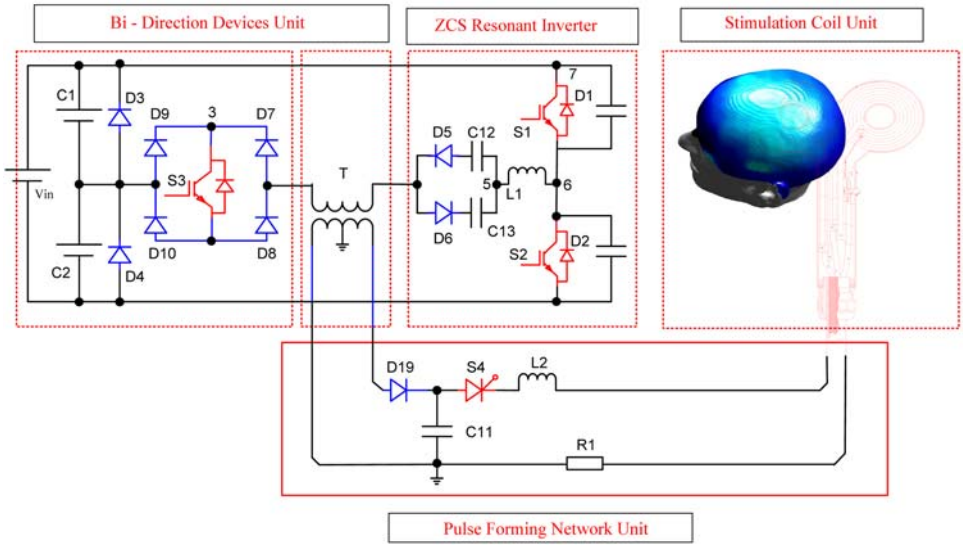

Fig. 1. (Color online) Transcranial magnetic stimulation actualized in the resonant converter method.

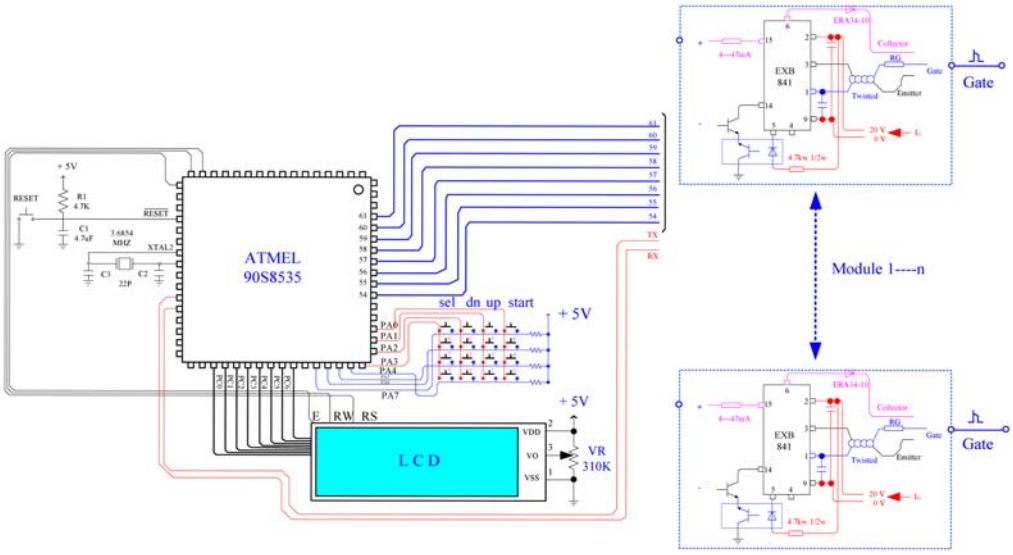

Fig. 3. (Color online) Circuit for operating and controlling element through composition of AVR 90S8535 one-chip microprocessor of ATMEL Company.

flows through D_3 and D_6. Current flowing in L_r is maximized when the C_r bi-voltage is 0.5 V_s, and Cr bi-voltage is maximized to become identical to Io after current flowing in L_r exceeds the peak. Stage 3 ends at t_3, when IGBT-1 is turned on. Figure 2 presents a circuit for monitoring output and an output sensor of charge-discharge device through the capacitor.

2.2. Control Devices

Fig. 3 operates element through composition of AVR 90S8535 one chip microprocessor of ATMEL company and presents control circuit. The AVR 90S8535 one chip microprocessor simply manages operations and the delay time control circuit function. The control circuit is largely composed of three parts. One part is the keyboard that receives input of operated delay time. The second part is the FND (multi-segmented LED displays) display component that displays input delay time, and the last part is the AVR 90S8535 one-chip microprocessor, the most essential part in this control circuit. The actions of this control circuit follow. Input of delay time information through the keyboard was transmitted to the AVR 90S8535 one-chip microprocessor, and three different signals were released by the program decided by the AVR 90S8535 one chip. We designed and produced in simple composition, such as IGBT, one-chip microprocessor, and pulse transformer for actualizing simpler and accurate device when compared with the previous transcranial magnetic stimulation.

Fig. 4 presents the operation and control pulses that provide delay time function for operating transcranial magnetic stimulation that triggers the IGBT. Adjustment of the delay time was actualized using the one-chip microprocessor 90s8535. Operation of the delay time control circuit executes simultaneous signal input for operating the stimulation coil of the transcranial magnetic stimulation in the system and control circuit to release sine wave in AT90S8535 in time decided by R_1 and C_1 in input signal increase edge. When sine waves were re-entered in the AT90S8535, sine waves were released from AT90S8535 in time decided by R_2 and CE in lower edge of sine wave. This signal becomes the gate trigger signal for the operating IGBT. Thus, the delay time can be controlled by adjusting the AT90S8535 pulse range according to R_1 and C_1.

2.3. Stimulation

Fig. 5 presents computer simulated based on Fig. 1 and Fig. 2. The conditions were: L_r = 4.8 uH, C_r = 47 nF × 5, Lop = 4.8 uH, C_o = 60,000 μF, turn ratio = 1:3, and fs = 154 kHz. Large Link Cap is unfavorable for phase but modest effect is provided in noise aspect or output volt-

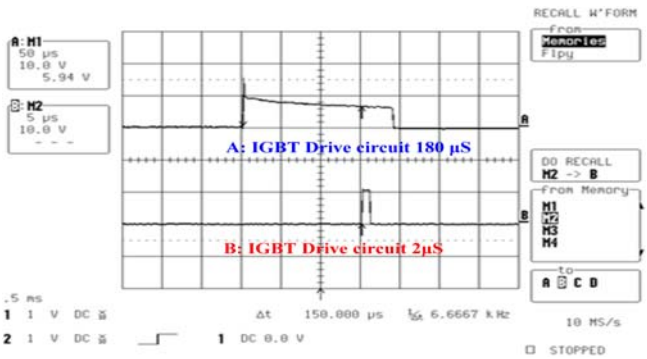

Fig. 4. (Color online) Operating and controlling pulse for providing regular delay time function, which manages transcranial magnetic stimulation for triggering IGBT.

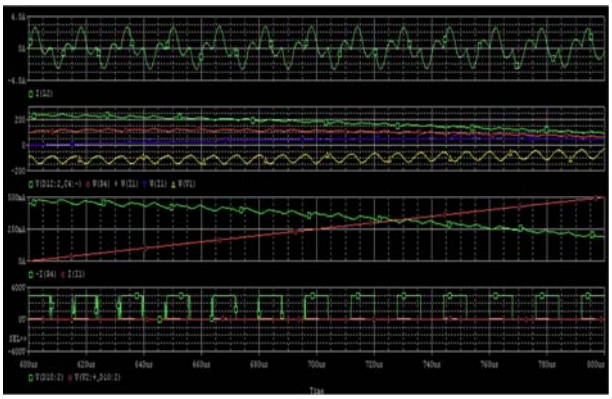

Fig. 5. (Color online) Computer simulation based on the half-bridge parallel-loaded resonant converter method.

age increase. Using the conditions L_r = 4.8 uH, C_r = 47 nF × 5, Lop = 4.8 uH, C_o = 60000 μF, turn ratio = 1:3, f_s = 154 kHz, and C_{12} = 330 μF, output voltage increased by 2.5 V for 20 ms, noise and peak of voltage and current decreased, and phase decreased through dispersion of input current in the frontal area of sine waves. Although it was assumed that output voltage increase would be accelerated through an increase in transformer turn rate, it was shown that voltage increase speed decreased as secondary current decreased according to increase in turn rate. For L_r = 4.8 uH, C_r = 47 nF × 5, Lop = 4.8 uH, C_o = 60,000 μF, turn ratio = 1:6, f_s = 154 kHz, and C_{12} = 330 μF, output voltage increased by 1.4 V for 20 ms. Although final voltage decreased with a decrease in transformer turn rate, supply can be achieved to 350 V, and a decrease in turn rate is favorable because the secondary voltage supply ability increases.

For L_r = 4.8 uH, C_r = 47 nF × 5, Lop = 4.8 uH, C_o = 60,000 μF, turn ratio = 1:2, f_s = 154 kHz, and C_{12}= 330 uf, output voltage increased by 3.5 V for 20 ms, primary and secondary current stress increased slightly with an increase in supplied electric capacity, and resonant frequency is decided as L_r, C_r and $C_{10,11}$ to present calculated value as 159 kHz when transformer, Lop, output condenser are neglected. For L_r = 4.8 uH, C_r = 47 nF × 5, Lop = 4.8 uH, C_o = 60,000 μF, turn ratio = 1:2, f_s = 159 kHz, and C_{12}= 330 μF, output voltage increased by 3.7 V for 20 ms, and switching frequency did not completely coincide with the resonant frequency when the waveform was expanded. The waveform was similar to the below-resonant operation waveform, and the output voltage increased when resonant frequency was approached due to a slight increase in switching frequency. For L_r = 4.8 uH, C_r = 47 nF × 5, Lop = 4.8 uH, C_o = 60,000 μF, turn ratio = 1:2, f_s = 170 kHz, and C_{12} = 330 μF, output voltage increased by 5.2 V for 20 ms, and primary and secondary current stresses and noise increased due to an increase in the supplied electric capacity. Switching frequency was increased to operate in above-resonant mode. Output voltage increased by 10 V during L_r = 4.8 uH, C_r = 47 nF × 5, Lop = 4.8 uH, Co = 60,000 μF, turn ratio = 1:2, f_s = 200 kHz, C_{12} = 330 μF, 20 ms, primary and secondary current and voltage stress were greatly increased, and parts without resonation were generated. Resonated areas presented as above-resonant mode and waveforms adjacent to resonant frequency during expansion of waveforms. The increase in output voltage was accelerated when the input/output conversion ratio increased with an increase in Q value.

3. Experimental Results

Design is achieved to provide considerable tolerance in order to guarantee transformer motions regarding rapid input change and output change in the application of power device. Since loss generated from core hysteresis increases with a larger change in magnetic flux, it is useful to maintain small changes of magnetic flux. However, because increase in turn rate is continued to increase in conductivity loss, optimum design for minimizing total loss is achieved. Fig. 6 presents a charged waveform during 125.6 kHz switching frequency, and it presents the experimental waveform used when A was 20 mS 100 V, B was 20 μs 20A, and C was 20 mS 400 V. Input voltage of the transformer can near bi-voltage of resonant condenser and interpretation can be achieved for each section. Fig. 7 presents a charged waveform during 127.2 kHz switching frequency, and it presents a measurement waveform when A was 20 mS 100 V, B was 20 μs 20 A, and C was 20 mS 200 V. Since the secondary voltage of the transformer was limited to output voltage, the secondary turn rate can be calculated.

Fig. 8 illustrates the charged waveform during 112.8 kHz switching frequency, and the experimental waveform

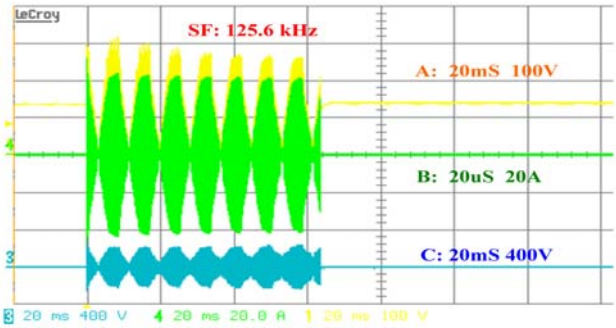

Fig. 6. (Color online) Charged waveform during 125.6 kHz switching frequency, and the experimental waveform during 20 mS 100 V of A, 20 μs 20 A of B, and 20 mS 400 V of C.

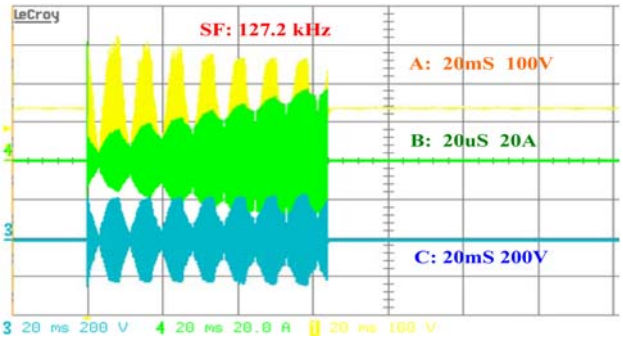

Fig. 7. (Color online) Charged waveform during 127.2 kHz switching frequency, and the experimental waveform during 20 mS 100 V of A, 20 μs 20 A of B, and 20 mS 200 V of C.

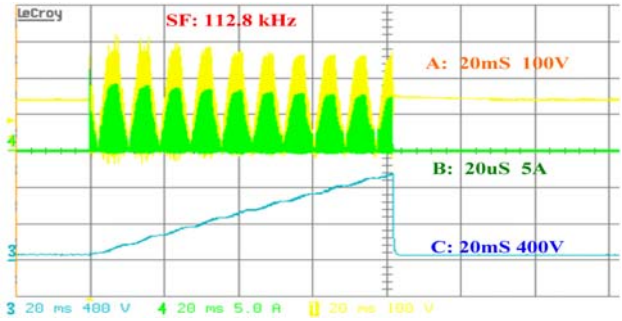

Fig. 8. (Color online) Charged waveform during 112.8 kHz switching frequency, and the experimental waveform during 20 mS 100 V of A, 20 μs 5 A of B, and 20 mS 400 V of C.

is presented when A was 20 mS 100 V, B was 20 μs 5 A, and C was 20 mS 400 V. Assuming that maximum output voltage is the switching half-period, and material of 3,000G saturated magnetic flux density is assumed to be used, ± 2,000G is possible when observing half-bridge characteristics. If switching frequency is greater than 100 kHz, use under ± 1,500G is reasonable, thus it was set to 3,000G. As can be observed from simulation results, the turn rate, final voltage, and voltage increase speed correlate. Fig. 9 presents a charged waveform during 112.8 kHz switching frequency, and an overlapping measurement waveform existed when A was 20 mS 100 V, B was 20 μs 5 A, and C was 20 mS 400 V. The copper area was determined by the size of the cross-sectional area in the flowing current used by the transformer. The quantity of electricity supplied during charge/discharge can be obtained by measuring the quantity of the output condenser and voltage change range. Average current value can be calculated by dividing the charge/discharge repetition time, and secondary RMS current value can be maintained. Since the resonating inductor is the addition of primary projection value of output current and the resonating current, current value occupies the largest part. Fig. 10 presents

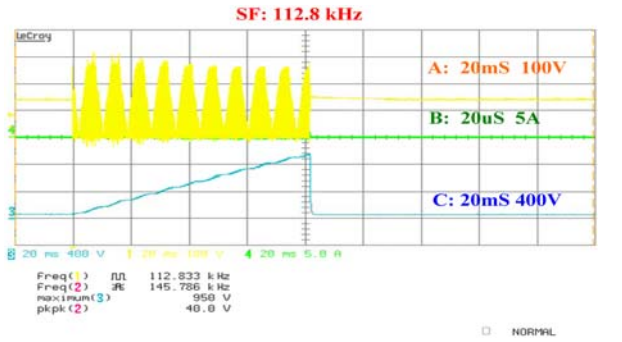

Fig. 9. (Color online) Charged waveform during 112.8 kHz switching frequency, and the measurement waveform overlapped during 20 mS 100 V of A, 20 μs A of BA, and 20 mS 400 V of C.

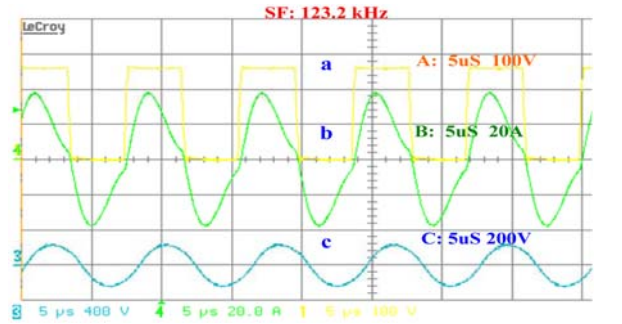

Fig. 10. (Color online) Charged waveform during 123.2 kHz switching frequency, and the experimental waveform during 5 μs 100 V of A, 5 μs 20 A of B, 5 μs 200 V of C.

the charged waveform during 123.2 kHz switching frequency, and it presents an experimental waveform when A was 5 μs 100 V, B was 5 μs 20 A, and C was 5 μs 200 V. Thickness of the coil is determined by frequency of the flowing current, and a coil with a radius less than its skin depth is generally selected. Equivalent cross-sectional area was composed of various coil strands in case of high frequency even when possessing the same

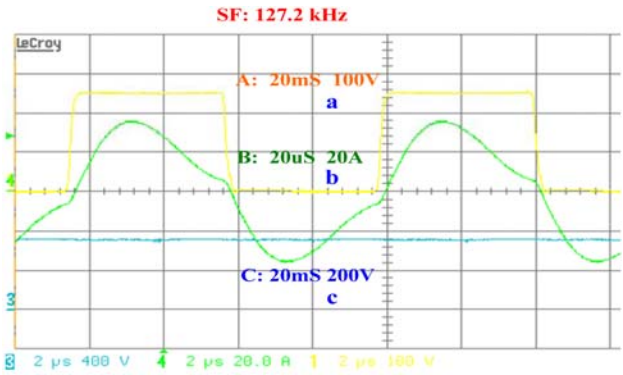

Fig. 11. (Color online) Charged waveform during 127.2 kHz switching frequency, and the measurement waveform during 200 mS 100 V of A, 20 μs 20 A of B, and 20 mS 200 V of C.

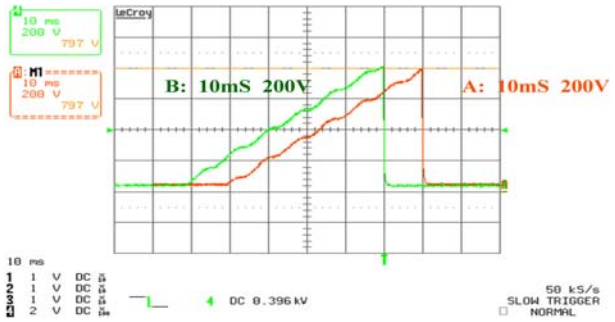

Fig. 12. (Color online) Charged waveform during 10 mS 200 V of A and 10 mS 200 V of B.

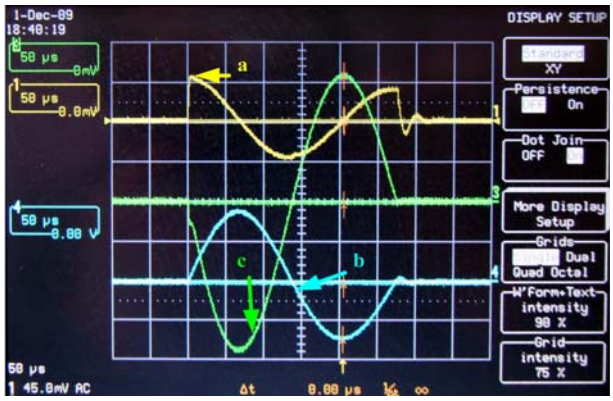

Fig. 13. (Color online) (A) The process of turning off in curve center in IGBT turn-on to turn on in the end, (B) the magnetic coil current, and (C) the capacitor discharge current of the precise discharge function.

current value. Fig. 11 presents the charged waveform during 127.2 kHz switching frequency, and it presents the measurement waveform when A was 200 mS 100V, B was 20 μs 20 A, and C was 20 mS 200V. Fig. 12 presents the charged waveform when A was 10 mS 200V and B was 10 mS 200 V. In Fig. 13 a is the process of turning off in curve center in IGBT to turn on in the end, b is the magnetic coil current, and c is the capacitor discharge current of precise discharge function.

4. Conclusion

This study designed and produced a device by introducing the switching technique of the half-bridge parallel load method in order to easily control the electric charge/discharge in the capacitor and the free-form voltage and current pulse. Transcranial magnetic stimulation was implemented and used to study characteristics. IGBT, AT90S8535, and a pulse transformer were used in switching of the half-bridge parallel load method to achieve a circuit composition of very simple structure. Charge-discharge control can be accurately and easily executed by operating through delay time of various voltages regarding stimulation coil operation. Minimum voltage released from the charge/discharge control presented 3.6 kV voltage possessing approximately μs pulse range. Delay time regarding operation of voltage stimulation coil possesses the variable range of 30 μs~3 ms. It was shown that a 10% speed increase and output expansion was achieved in transcranial magnetic stimulation with the half-bridge parallel load method compared to that of the previous device. Switching frequency was changed to detect charged waveforms, and various shapes of magnetic coil current were actualized through charge-discharge experiment by setting diverse repetition and delay time of IGBT turn-on, turn-off, turn-on process.

Acknowledgement

This work was supported by the Dong-A University Research Fund.

References

[1] V. Walsh, and A. Pascual-Leone, Transcranial Magnetic Stimulation: A Neurochronometrics of Mind, The MIT Press, Cambridge (2005).
[2] B. W. Wilson, K. Caputa, M. A. Stuchly, J. D. Saffer, K. C. Davis, C. E. Washam, L. G. Washam, G. R. Washam, and M. A. Wilson, Bioelectromagnetics **15**, 563 (1994).
[3] S.-S. Choi, J. Magnetics **16**, 246 (2011).
[4] Walter J. Levy, Roger Q., M. D. Cracco, Anthony T. Barker, and J. C. Rothwell, Magnetic Motor Stimulation: Basic Principles and Clinical Experience, Elsevier Science, Oxford (1991).
[5] Carl Senior, Tamara Russell, and Michael S. Gazzaniga, Methods in Mind, The MIT Press, Cambridge (2006).
[6] Pascal Wallisch, Michael Lusignan, Marc Benayoun, Tanya I. Baker, Adam Seth Dickey, Nicho Hatsopoulos, MATLAB for Neuroscientists: An Introduction to Scientific Computing in MATLAB, Academic Press (2008).
[7] Images William D. Penny, Karl J. Friston, John T. Ashburner, Stefan J. Kiebel, and Thomas E. Nichols, Statistical Parametric Mapping, Academic Press, San Diego (2006).
[8] R. S. J. Frackowiak, K. J. Friston, and C. Frith, HumanBrain Function. 2nd ed., Academic Press, San Diego (2003).
[9] Sun-Seob Choi, Treatment pulse application for Magnetic Stimulation, Journal of Biomedicine and Biotechnology, **2011**, 278062 (2011).
[10] Orrin Devinsky, Aleksandar Beric, and Michael Dogali, Electrical and Magnetic Stimulation of the Brain and Spinal Cord, Raven Press, New York (1993).
[11] Mark S. George and Robert H. Belmaker, Transcranial Magnetic Stimulation in Clinical Psychiatry, American Psychiatric Publishing, Inc., London (2006).
[12] D.-H. Ha, J. Magnetics **16**, 234 (2011).